# Optimal Parameters Design for Manufacturability under Unknown Feasibility Constraints

Guoyan Li[1], Xiaoning Jin[1], Yujia Wang[2] and Swastik Kar[3]

2023 IEEE 19th International Conference on Automation Science and Engineering (CASE) | 979-8-3503-2069-5/23/$31.00 ©2023 IEEE | DOI: 10.1109/CASE56687.2023.10260375

***Abstract*— This paper proposes a novel approach for optimizing the manufacturing process under unknown feasibility constraints. Due to the complex interdependencies among the numerous design of experiment parameters, a trial-and-error approach is impractical. Our approach combines a predictive modeling block that uses two machine learning models and an experimental design component employing multiple sampling strategies. We applied this method to the synthesis of 2D material via thermal chemical vapor deposition and achieved optimal material quality within only 7 batches of experiments, amounting to 61 samples. Additionally, we successfully identified the feasible region of synthesis parameters necessary for producing the desired material. These results not only highlight the effectiveness of our method but also its potential to guide engineers towards the most desirable outcome in manufacturing process optimization.**

## I. INTRODUCTION

Exploring the manufacturability of materials through a process often involves conducting numerous experiments with varying process parameters. However, this approach can be both costly and inefficient as it requires significant efforts to collect large amounts of data from experiments. The traditional design of experiments (DoE) methods such as factorial and Latin Hypercube design (LHD) [1] are commonly used for manufacturability analysis and optimal parameters design. For manufacturing processes with partially or completely unknown physics, the connection between process parameters and quality is frequently nonlinear and nonstationary. This complexity poses a challenge for DoE methods that rely on statistical principles to function effectively.

There has been a growing interest in the use of machine learning (ML) methods for optimizing manufacturing processes, including mechanical design [2] and material discovery [3]. Specifically, recent studies in manufacturing process analysis have focused on developing ML-based surrogate models that use historical datasets to establish data-driven processing-property linkages. Recent work [4] applied the Support Vector Regression model in the selective laser melting (SLM) process to analyze the relationship between the process parameters and the three responses. Support Vector Machine (SVM) classification and regression models were utilized in [5] to find the region of the design space that yields quantum-confined nanoplatelets and predict the thickness of quantum-confined CsPbBr3 nanoplatelets. Previous ML-assisted methods in manufacturing require a substantial amount of experimental data as training data. This passive approach lack of control over the process and may result in prediction error due to limitations in the size and quality of the training data. To overcome this significant challenge, recent research efforts have shifted towards utilizing active learning (AL) or optimal experimental design. This enables an iterative procedure to obtain a surrogate model with minimal manual effort. Research work [6] proposed an active learning method to support In-situ process monitoring in additive manufacturing.

Under the active learning framework, Bayesian optimization (BO) frameworks have also been applied for experimental design. The BO framework also involves a closed loop where predictions from the current machine learning model guide the subsequent experimental design to refine the ML model iteratively as new experiments are implemented. The difference between the AL and the BO is that the objective of the BO is to identify the global optimum with the fewest possible number of experiments. A sequence of samples was determined by the acquisition function via balancing the trade-off between exploitation (promising samples with the property close to the desired value) and exploration (regions of the experimental parameter space with high predictive uncertainty). BO algorithm has been successfully applied in nanotube synthesis [7], polymer fiber materials synthesis [8], and control of laser wakefield accelerators [9].

However, in real industrial applications, the optimization process always encounters physical constraints that restrict the experimental design and process optimization. There are two types of physical constraints: 1) parameter constraints and 2) quality constraints. However, owing to the complex relations in nonlinear multivariate design space, physical constraints of quality are usually unknown that can only be known once the experiments are evaluated. For example, the overall design space in simulation-based mechanical design [11], the overall design space can be divided into two regions: the feasible region and the unfeasible region where the objective function values do not exist because the simulation has failed to converge. Incorporating constraints of feasibility is significant to the success and accuracy of surrogate ML models.

In this work, we proposed a novel optimal parameter design approach under an unknown feasibility constraint of process parameters. The designed approach utilizes a closed-loop framework consisting of two components: 1) a predic-

[1]Department of Mechanical and Industrial Engineering, Northeastern University, Boston, Massachusetts, 02115, USA {li.guoy,xi.jin}@northeastern.edu

[2]Department of Chemical Engineering, Northeastern University, Boston, Massachusetts, 02115, USA wang.yujia1@northeastern.edu

[3]Department of Physics, Northeastern University, Boston, Massachusetts, 02115, USA S.Kar@northeastern.edu

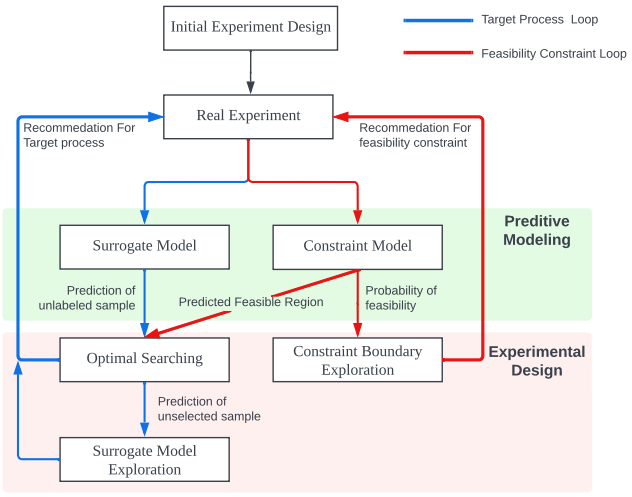


Fig. 1. The overview of proposed approach

tive modeling part that captures the relationships between process parameters and a target quality of interest, taking into account of feasibility constraints. 2) an experimental design part to recommend the next round of experiments via multiple sampling strategies. The overview of the proposed approach illustrated in Fig.1

The proposed predictive modeling block includes two parts: 1) a constraint model aims to capture the relationship between process parameters and the feasibility of samples. 2) a surrogate model aims to quantify how much information each unlabeled sample carries on for target process optimization. Different from traditional methods adopting a constrained Bayesian optimization framework where recommend next-round experiments via constrained expected improvement acquisition function [12], our approach successfully optimizes the target process and explores the boundary that distinguishes feasible experiments and infeasible experiments simultaneously. The main contributions of this paper are summarized as follows:

1) We proposed a novel optimal parameter design paradigm that not only optimizes the target quality of interest but also learns a boundary to distinguish feasible design space and unfeasible design space.
2) We developed an experimental design method via three sampling strategies to identify a batch of the most informative samples for the next-round experiment.
3) Our proposed framework has the potential to be applied to various manufacturing process that have feasibility constraints.

The remainder of the paper is organized as follows: Section II discusses the proposed optimal parameter design approach. A case study of a 2D material synthesis process is implemented and validated in Section III. Finally, a brief summary is provided in Section IV.

## II. PROPOSED APPROACH

This section presents the proposed optimal parameter design approach to optimize manufacturing processes that have unknown feasibility constraints. Two machine learning models adopted in the predictive modeling part are listed in II-B and II-C. The details regarding the parallel sampling strategy employed in the experimental design are presented in II-D

### A. Problem Definition

Consider a manufacturing process defined over a predefined parameter space $\mathscr{X} \subseteq \mathbf{R}^D$, where $\mathscr{X}$ is a space of process parameters. The process includes a target function $f : \mathscr{X} \to \mathbb{R}$, which we want to optimize, and a constraint function $h : \mathscr{X} \to \mathscr{C} = \{0,1\}$, related to the feasibility of parameter settings, which is assumed to be independent of $f$. For any experimental point $x = [x_1, \cdots, x_D]^\top \in \mathscr{X}$, the process will be feasible when

$$h(x) = 0 \tag{1}$$

and infeasible otherwise. For example, $f$ can be a surface roughness of mechanical structure given on design parameter vector $\mathbf{x}$, and $h$ can be the boundary to classify the success and failure of the experiments given on the same design parameter vector $\mathbf{x}$. To find the optimal parameter $\mathbf{x}^*$ within feasible space, which can be regarded as a constrained optimization problem in turn

$$\begin{aligned} \min_{x \in \mathbf{X}} \quad & f(x) \\ \text{s.t.} \quad & h(x) = 0 \end{aligned} \tag{2}$$

Here we assume both functions can only be observed or evaluated with costly real experiments or relevant physics-based models. The feasible region $\mathscr{X}_s$, the subset of parameter space with successful settings, is unknown and difficult to obtain owing to the high cost, such as experimental time and cost. We refer to the complementary of the feasible region as the infeasible region such that $\mathscr{X}_f = \mathscr{X} \backslash \mathscr{X}_s$. Suppose we have $n$ observed samples from the design space denoted by $\mathbf{X}_n = \{\mathbf{x}_i\}_{i=1}^n$. $\mathbf{C} = [c_1, c_2, \cdots, c_n]$ represent the feasibility label and a set of observed feasible samples denoted by $\mathbf{X}_m = \{\mathbf{x}_m\}_{i=1}^m$. $\mathbf{Y} = \{y_1, y_2, \cdots, y_m\}$ represent the corresponding quality outputs of feasible samples $\mathbf{X}_m$. We refer to the complementary of feasible experiments as the infeasible experiments set such that $\mathbf{X}_f = \mathbf{X}_n \backslash \mathbf{X}_m$. $\mathbf{X}_u = [x_1, \ldots, x_u]$ represents all unlabeled data. In this work, we assume that the surrogate model $f$ for estimating the target function value follows a Gaussian Process (GP) prior.

$$f \sim \mathscr{GP}(\mu_f(\cdot)), k_f(\cdot)) \tag{3}$$

where $\mu_f(\cdot)$ is a mean function and $k_f(\cdot)$ is a covariance kernel function [13].

### B. Constraint Model for Feasibility Estimation

In this optimal parameter design approach, we begin by utilizing a constraint model, which is a binary classification model trained through a graph-based semi-supervised classification method on a dataset containing a small number of labeled data points and a large number of unlabeled data points. This constraint model is utilized to explore the

feasibility of data. With the help of this constraint model, the parameter space can be naturally divided into two distinct regions: 1) the feasible region, where experiments yield successful outcomes, and 2) the infeasible region, where data indicate undesirable manufacturing outcomes. We opt graph-based semi-supervised learning (GSSL) model in this study is that GSSL models are effective when the size of the training dataset is small[14]. Especially in the material science domain, data scarcity is the most prevalent issue in ML-assistant material science research.

The first step of GSSL is to construct a graph from all labeled and unlabeled samples, where each sample is represented by a vertex in the weighted graph that measures the similarity between each sample. In this study, the similarity of each sample is measured by $W_{i,j} = exp(\frac{-|x_i - x_j|^2}{\sigma})$, where $\sigma$ is a hyperparameter of this Gaussian kernel function. Then the labels of those unlabeled samples can be propagated by exploiting the label dependency information extracted from available label information. Our constraint model is similar to the Local and Global Consistency (LGC) algorithm, and details of the LGC model can be found in the [15]. We refer to $P$ as a vector of the probability of the predicted label of the constraint model. The predicted feasibility label $c_*$ of an unlabeled sample $x_*$ is defined as follows,

$$\arg\max_{c_*} P(c_*|x_*, \mathbf{X_n}) \tag{4}$$

### C. Surrogate Model for Target Process Optimization

In the second part of the predictive modeling block, we choose Gaussian Process Regression (GPR) model to learn our target function $f$, which captures the relationship between parameters and target process quality. The objective of the GPR model here is to learn a specific mapping function $f(x)$, which maps an input vector to a label value and a Gaussian prior distribution is placed over $f$. That is

$$p(f|X_m) \sim \mathcal{N}(f|\mu_m(x), K_m(x,x')) \tag{5}$$

where $\mu_m(x)$ is mean function and $K_m$ is an $m \times m$ is a covariance matrix and the element of $K_m$ is built via a kernel function $k(x,x')$. In this work, we consider the automatic relevance determination using the Matern52 kernel function, which is parameterized in terms of the kernel parameters in vector $\theta = [\sigma_f, \sigma_l]$

$$k(x_i, x_j|\theta) = \sigma_f^2(1 + \sqrt{5}r + \frac{5}{3}r^2)\exp(-\sqrt{5}r) \tag{6}$$

where

$$r = \sqrt{\sum_{l=1}^{d} \frac{(x_{il} - x_{jl})^2}{\sigma_l^2}}$$

In kernel function (6), $\sigma_f$ is a non-negative over scale hyperparameter and $\sigma_l$ is a different non-negative length hyperparameter for each predictor. The kernel parameter vector $\theta$ is unknown initially, and the optimal $\theta$ given on observed experiments $\mathbf{X}_n$ can be estimated by maximizing the marginal likelihood via L-BFGS-B optimizer [16], which are

$$l(y_m|X_m, \theta) = -\frac{1}{2}\mathbf{y}^T\mathbf{K}_m^{-1}\mathbf{y} - \frac{1}{2}\log \mid \mathbf{K}_m \mid + \frac{1}{2}\log 2\pi \tag{7}$$

Given the observed experimental data and optimal parameter vector $\theta$, the prediction distribution of the latent function $f_*$ for an unlabeled data $x_*$ is

$$p(f_*|x_*, \mathbf{X}_m, \mathbf{y}_m) = \mathcal{N}(\mathbb{E}(\hat{f}(x_*)), \mathbf{Var}(\hat{f}(x_*))) \tag{8}$$

where

$$\mathbb{E}(\hat{f}(x_*)) = \mathbf{k}(x_*, \mathbf{X}_m)K_m^{-1}\mathbf{y}_m \tag{9}$$

$$\mathbf{Var}(\hat{f}(x_*)) = k(x_*, x_*) - \mathbf{k}(x_*, \mathbf{X}_m)K_m^{-1}\mathbf{k}(x_*, \mathbf{X}_m)^\intercal \tag{10}$$

### D. Parameter Design for Next Round Experiment

In this experimental design block, we designed a query generator via three different sampling strategies. Our query generator utilizes the prediction of unlabeled data from the predictive modeling block to select a group of informative unlabeled data for the next iteration.

**Pure exploration for constraint boundary** - To estimate the feasibility constraint of parameters, we utilized an active learning procedure that recommends unlabeled data with the highest uncertainty in the prediction. To measure the uncertainty of prediction for unlabeled data, we calculate the difference in prediction probability for binary class labels, which is defined as follows:

$$U(x_u) = 1 - \mid P(c_u = 0|x_u) - P(c_u = 1|x_u) \mid \tag{11}$$

where $P(c_u = 0|x_u)$ is the probability of the predicted feasible label,$P(c_u = 1|x_u)$ is the probability of the predicted infeasible label. The sample with the largest value of uncertainty, denoted as $U(x_u)$, is selected for recommendation in each iteration of the active learning procedure. The objective of this pure exploration process is to refine the classification boundary of the constraint model, providing a more robust classifier to separate parameter space.

**Pure exploration for surrogate model** - To improve the reliability of the surrogate model for the target process, we recommend another group of samples with high uncertainty in the prediction for updating the model. Different from the classification problem, in the regression problem, the uncertainty of prediction is measured by the posterior variance of the surrogate model. We select unlabeled data where the posterior variance $\sigma(x_u)$ calculated using Equation (10) is maximized. By selecting these data, we can further refine the surrogate model and improve its predictive accuracy

**Acquisition function in BO recommendation** - In order to optimize the target process function, another sample is recommended via the traditional Bayesian optimization framework where an acquisition function is constructed to quantify the most informative candidate samples for next round experiment. Acquisition functions are usually derived from the $\mu(x_u)$ calculated by Equation (9) and $\sigma(x_u)$ calculated by Equation (10). This acquisition function allows a balance between exploitation (the predicted quality is high) and exploration (the posterior variance is high). Traditionally,

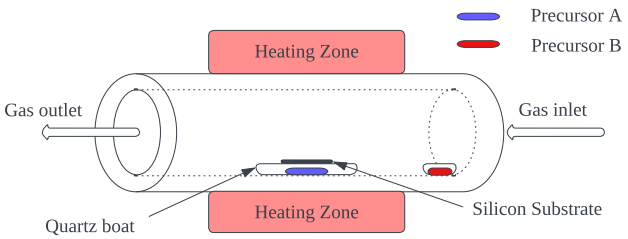


Fig. 2. Schematic diagram of the chemical vapor deposition apparatus.

the global maximum value of the acquisition function is selected. In this study, we adopt the Lower Confidence Bound (LCB) function as an acquisition function because we want to minimize our objective function, which is defined as follows:

$$x_t = \arg\max_{x_u} -\mu(x_u) + \beta\sigma(x_u) \tag{12}$$

where $\beta$ is a hyperparameter that controls the trade-off between exploration and exploitation. The $\beta$ in this work is predefined as a constant $\beta = 100$ based on the scale of $\mu(x_u)$ and $\sigma(x_u)$.

## III. Case Study: 2D Material Synthesis Via Chemical Vapor Deposition Method

Since their modern debut in 2004, 2-dimensional (2D) materials have continued to exhibit scientific and industrial promise, providing a broad materials platform for scientific investigation and development of nano- and atomic-scale devices. Chemical vapor deposition (CVD) is a scalable technology that is widely used for the synthesis of high-quality 2D materials, including graphene and transition metal dichalcogenides (TMDCs). A schematic diagram of the CVD apparatus is shown in Fig. 2. However, the synthesis of high-precision 2D materials via the CVD method requires a larger number of experiments to investigate how changing various synthesis parameters like time, pressure, and flow rate impact the quality and reliability of the synthesized 2D materials. But with increasing complexity in material synthesis, the combination possibilities become too large for trial-and-error approaches to be practical and economic. In this study, we optimize a material synthesis via the CVD process via the proposed optimal parameter design method.

### A. Experimental Setting

In this study, we focus on adjusting five correlated synthesis parameters to achieve high-quality 2D material. These five parameters form a 5-dimensional design space with 384 points for experiments and these five parameter range is shown in Table I. The range of each parameter is predefined by material scientists according to domain knowledge. Our 2D materials are grown on a 1cm$\times$1cm silicon substrate and two precursors are separately placed in two alumina boats. In our synthesis process, two distance parameters are involved: $D_a$ measures the distance between the boat of precursor A and the right edge of the heating zone, while $D_b$ measures the distance between the boat of precursor B and the temperature

TABLE I

2D material synthesis input parameters space.

| Parameter | Kind | Range | Unit |
|---|---|---|---|
| $D_a$ | discrete | [14,16] with interval 1 | cm |
| $D_b$ | discrete | [12,15] with interval 3 | cm |
| F | discrete | [0.14, 0.23] with interval 0.03 | L/min |
| R | discrete | [5,20] with interval 5 | °c /min |
| T | discrete | [10,25] with interval 5 | min |

sensor. The temperature range for the synthesis process was set to a fixed range, and the ramp rate denoted by $R$ indicates the speed of temperature change from the lowest temperature to the highest temperature. Once the temperature reaches its highest value, we wait for another $T$ minutes before cooling down the tube and collecting the sample, which is brought down to room temperature. The gas flow rate through the tube is represented by the parameter $F$.

On the other hand, layer-dependent features extracted from photoluminescence (PL) spectra or Raman Spectroscopy are widely used as an indicator to represent the quality of 2D materials [17], [18]. In this study, we measure the quality of 2D materials using the fitted half-maximum peak (FWHM) width of the excitonic peak of PL spectra obtained from successful experiments. A smaller FWHM width indicates higher material quality. An example of PL spectra is shown in Figure 3. We usually can collect multiple PL spectra

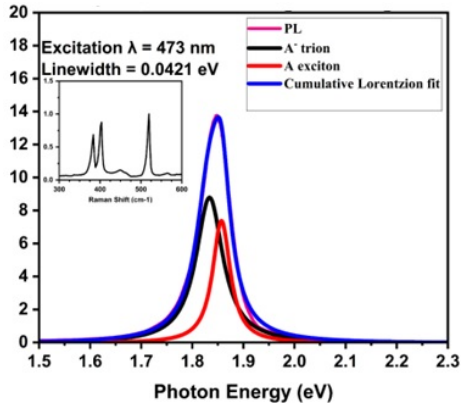


Fig. 3. An example of normalized PL spectra by the in situ Raman peak of the 2D material substrate at 521 cm-1 and its A exciton and A-trion peak fitted by the Lorentzian function from OriginLab software are shown in Figure 3. The FWHM width of the excitonic peak (represented by the red line in Figure 3) is used as our optimization objective.

on a single 1cm $\times$ 1cm silicon substrate and choose the smallest FWHM width from each sample to serve as our target quality vector $\mathbf{Y}$. If we can not collect PL spectra from a silicon substrate, the corresponding parameter setting is unfeasible. We treat the conditions that can grow target material as a constraint in our experimental design. Our feasibility constraint classifies the overall design space into two regions: 1) feasible region where 2D material can grow and 2) infeasible region where 2D material can not grow. By uncovering the relationship between synthesis parameters and experimental success, we aim to help material scientists

establish experimental conditions with a high success rate. The objective of this study is to identify optimal parameter settings that result in target 2D material with a minimal FWHM width and to develop a classification boundary to distinguish between feasible and infeasible samples.

### B. Initial Design and Iterative Selection Process

In this study, we employ a pool-based active learning process on a finite candidate pool of synthesis parameters, as defined in Table I. We begin by selecting an initial training dataset of 26 experiments without replacement from the candidate pool. Our initial selection strategy consists of two methods. Firstly, we collected 14 samples based on material scientists' domain knowledge. Secondly, we use Taguchi methods [1] to select the second part of the initial design, consisting of 12 samples downscaled from orthogonal arrays generated for the whole parameter design space. This initial design, which combines the traditional design of experiments (DoE) methods with chemical domain knowledge, is intended to provide a more informative starting point for our approach than an initial design generated from a single method. It can also be used as a warm-start for our approach. Our initial training dataset $D_l$ is obtained after conducting these experiments.

In this study, we set the batch size to 5, and we recommend a total of 5 points in each iteration. We select two points with the highest value of $U(x_u)$ for constraint exploration and two points with the highest value of $\sigma(x_u)$ for surrogate model exploration. An additional point is obtained using Equation (12) to find a sample with lower FWHM width. These five selected points are then removed from the candidate pool and incorporated into the training dataset after conducting experiments for the next iteration. This sequential alternation between recommendation and experiment is repeated until we meet our termination criteria. In this study, we terminated our experiments at the $10^{th}$ iteration.

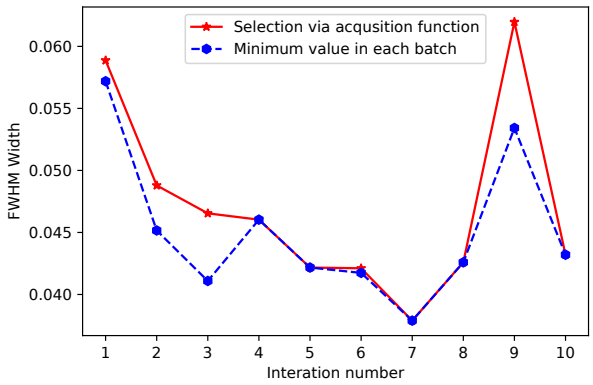


Fig. 4. Red line is the distribution of FHWM width measurements from each sample proposed by the design acquisition function. Blue dash line is the distribution of minimum FHWM width measurements in each batch samples proposed by three sampling strategies in total

### C. Results and Discussion

In each iteration group, the system suggests one point to optimize synthesis and the other four via active learning strategies to enhance the robustness of the constraint model and surrogate model. To demonstrate the progress of the framework during each iteration, The red in Fig. 4 shows the FWHM width of each sample recommended based on the designed acquisition function, which indicates the decrease in FWHM width as the iteration number of experiments increases before the $7^{th}$ iteration. In order to prove that we obtained the optimal parameter setting in the $7^{th}$ iteration, three more iterations were conducted.

Meanwhile, our optimal parameter approach can also be treated as a batch-mode Bayesian optimization framework. The blue dash line in Fig. 4 shows the minimum FWHM width of five recommendations in each iteration, which also indicates the same trend as red line shown in Fig. 4. Overall, our approach successfully optimizes the synthesis process.

In this proposed framework, the second objective is to estimate the feasibility boundary that disseminates the feasible points and infeasible points. After iteration $10^{th}$, we will obtain a constraint model trained with all labeled points. This constraint model will also guide synthesis parameter control. Fig. 5 shows the contours of the predicted growth probability of design space.

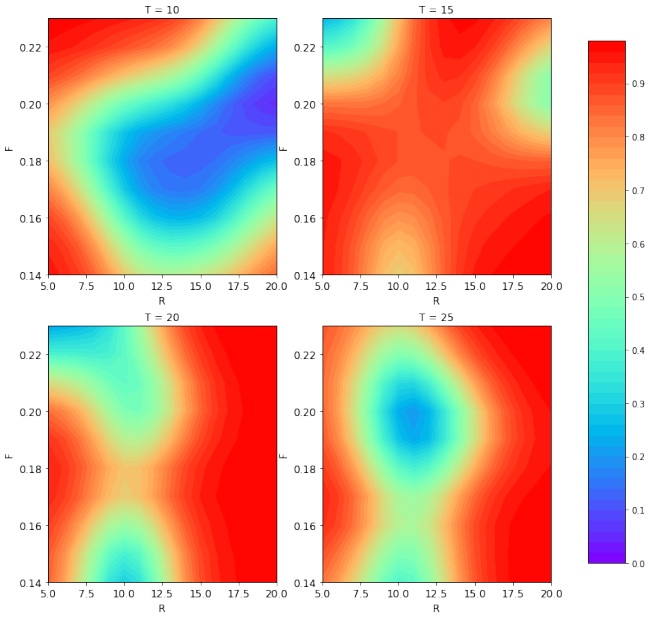


Fig. 5. Prediction from constraint model in terms of growth probability is shown as a contour plot. The synthesis parameter $D_a$ and $D_b$ were held constant at 16cm and 15cm, which are the optimal setting as the optimal sample obtained in the $7^{th}$ iteration

### D. Algorithm Validation

Before the optimization process starts, we train our constraint model via our 26 initial selection samples, which include 9 success samples and 17 failure samples, and all unlabeled synthesis parameters. Owing to the limited

labeled data, to test the performance of our initial constraint model, the leave-one-out cross-validation method was used to validate our constraint predictor. The predicted accuracy of the initial constraint model is 91.05%.

To validate the performance of our constraint model after the $10^{th}$ iteration, we selected 10 points from the remaining unlabeled data, where five of them were randomly selected and another five points with the least predicted FWHM width obtained from the surrogate model. We use these ten samples' experimental results as the validation study to confirm that our constraint model is able to capture the feasible region accurately. Within these ten iterations, no unfeasible points were misclassified as feasible points. The

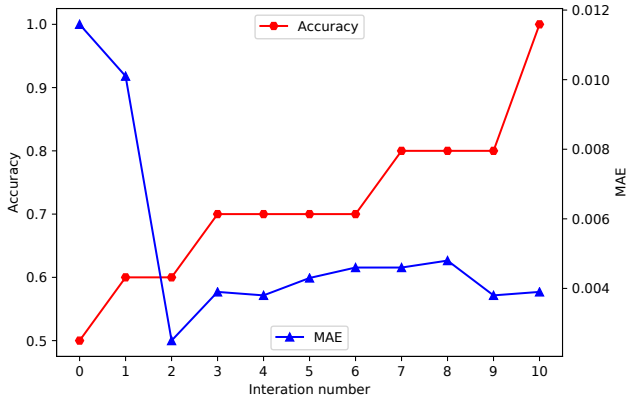


Fig. 6. Performance of constraint model and surrogatem model in each iteration

red line in Fig.6 depicts the accuracy of the prediction from the constraint model in each iteration. Meanwhile, we also evaluate the performance of our surrogate model. The mean absolute error (MAE) is used to measure the performance of the surrogate model for these ten points. Our surrogate model achieves an MAE of 0.0039 in the $10^{th}$ iteration. The MAE under different iterations is shown in the blue line in Fig.6. Here we can only evaluate the predicted FHWM width when this point is classified as a feasible point.

## IV. CONCLUSIONS

In this work, we proposed an optimal parameter design approach under an unknown feasibility constraint. Our proposed method comprises a predictive modeling block that employs two machine learning models. A constraint model is utilized to estimate the feasibility constraint, while a surrogate model is employed to establish the relationship between process parameters and product quality. Furthermore, a parallel sampling strategy based on three selection criteria is proposed to guide iterative experimentation. Through a case study on 2D material synthesis via the CVD process, our proposed approach has been validated and has demonstrated the effectiveness of process optimization and the robustness of feasibility estimation. By conducting 61 out of 384 possible trials, our method has obtained the optimal parameter setting, which constitutes 16% of the overall parameter space. In this work, we focus on the discovery of optimal parameters and we don't have a fully labeled dataset supporting comparison of benchmark models. For future work, we will investigate the robustness of the method by using a different number of intial trials and compare the performance of optimization with other ML-based parameter design methods in manufacturing.

## ACKNOWLEDGMENT

This material is based upon work partially supported by the National Science Foundation under Grant No. 1943801 and TIER 1 seed funding by Northeastern University.

## REFERENCES

[1] Santner, Thomas J., et al. The design and analysis of computer experiments. Vol. 1. New York: Springer, 2003.
[2] Gongora, Aldair E., et al. "A Bayesian experimental autonomous researcher for mechanical design." Science advances 6.15 (2020): eaaz1708.
[3] Raccuglia, Paul, et al. "Machine-learning-assisted materials discovery using failed experiments." Nature 533.7601 (2016): 73-76.
[4] Li, Jingchang, et al. "A prediction approach of SLM based on the ensemble of metamodels considering material efficiency, energy consumption, and tensile strength." Journal of Intelligent Manufacturing (2022): 1-16.
[5] Braham, Erick J., et al. "Machine learning-directed navigation of synthetic design space: A statistical learning approach to controlling the synthesis of perovskite halide nanoplatelets in the quantum-confined regime." Chemistry of Materials 31.9 (2019): 3281-3292.
[6] Dasari, Siva Krishna, et al. "Active learning to support in-situ process monitoring in additive manufacturing." 2021 20th IEEE International Conference on Machine Learning and Applications (ICMLA). IEEE, 2021.
[7] Chang J, Nikolaev P, Carpena-Núñez J, Rao R, Decker K, Islam AE, et al. Efficient Closed-loop Maximization of Carbon Nanotube Growth Rate using Bayesian Optimization. Sci Rep 2020;10:1–9.
[8] Li, Cheng, et al. "Rapid Bayesian optimisation for synthesis of short polymer fiber materials." Scientific reports 7.1 (2017): 1-10.
[9] Shalloo, R. J., et al. "Automation and control of laser wakefield accelerators using Bayesian optimization." Nature communications 11.1 (2020): 6355.
[10] Roussel, Ryan, et al. "Turn-key constrained parameter space exploration for particle accelerators using Bayesian active learning." Nature communications 12.1 (2021): 5612.
[11] Tran, Anh, et al. "pBO-2GP-3B: A batch parallel known/unknown constrained Bayesian optimization with feasibility classification and its applications in computational fluid dynamics." Computer Methods in Applied Mechanics and Engineering 347 (2019): 827-852.
[12] Gelbart, Michael A., Jasper Snoek, and Ryan P. Adams. "Bayesian optimization with unknown constraints." arXiv preprint arXiv:1403.5607 (2014).
[13] Williams, Christopher KI, and Carl Edward Rasmussen. Gaussian processes for machine learning. Vol. 2. No. 3. Cambridge, MA: MIT press, 2006.
[14] Chong, Yanwen, et al. "Graph-based semi-supervised learning: A review." Neurocomputing 408 (2020): 216-230.
[15] Zhou, Dengyong, et al. "Learning with local and global consistency." Advances in neural information processing systems 16 (2003).
[16] Zhu, Ciyou, et al. "Algorithm 778: L-BFGS-B: Fortran subroutines for large-scale bound-constrained optimization." ACM Transactions on mathematical software (TOMS) 23.4 (1997): 550-560.
[17] Hejazi, Davoud, et al. "MoS2 Nanosheets with Narrowest Excitonic Line Widths Grown by Flow-Less Direct Heating of Bulk Powders: Implications for Sensing and Detection." ACS Applied Nano Materials 4.3 (2021): 2583-2593.
[18] Yue, Xiaowei, et al. "A wavelet-based penalized mixed-effects decomposition for multichannel profile detection of in-line Raman spectroscopy." IEEE Transactions on Automation Science and Engineering 15.3 (2017): 1258-1271